

See discussions, stats, and author profiles for this publication at: <https://www.researchgate.net/publication/24040483>

Extending the Range of Microsecond-to-Millisecond Chemical Exchange Detected in Labeled and Unlabeled Nucleic Acids by Selective Carbon R₁ρ NMR Spectroscopy

ARTICLE in JOURNAL OF THE AMERICAN CHEMICAL SOCIETY · MARCH 2009

Impact Factor: 12.11 · DOI: 10.1021/ja8091399 · Source: PubMed

CITATIONS

38

READS

29

4 AUTHORS, INCLUDING:



Anette Casiano-Negroni

University of Michigan

8 PUBLICATIONS 206 CITATIONS

SEE PROFILE

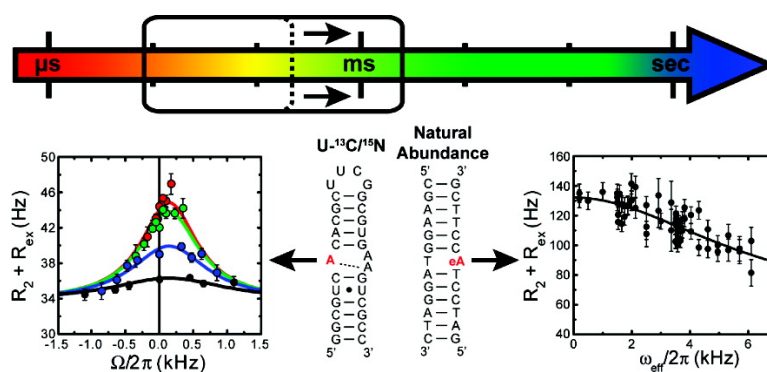
Communication

Extending the Range of Microsecond-to-Millisecond Chemical Exchange Detected in Labeled and Unlabeled Nucleic Acids by Selective Carbon R NMR Spectroscopy

Alexandar L. Hansen, Evgenia N. Nikolova, Anette Casiano-Negroni, and Hashim M. Al-Hashimi

J. Am. Chem. Soc., **2009**, 131 (11), 3818-3819 • DOI: 10.1021/ja8091399 • Publication Date (Web): 25 February 2009

Downloaded from <http://pubs.acs.org> on March 25, 2009



More About This Article

Additional resources and features associated with this article are available within the HTML version:

- Supporting Information
- Access to high resolution figures
- Links to articles and content related to this article
- Copyright permission to reproduce figures and/or text from this article

[View the Full Text HTML](#)



ACS Publications
High quality. High impact.

Extending the Range of Microsecond-to-Millisecond Chemical Exchange Detected in Labeled and Unlabeled Nucleic Acids by Selective Carbon $R_{1\rho}$ NMR Spectroscopy

Alexandar L. Hansen, Evgenia N. Nikolova, Anette Casiano-Negroni, and Hashim M. Al-Hashimi*

Department of Chemistry and Biophysics, University of Michigan, 930 North University Avenue, Ann Arbor, Michigan 48109

Received November 22, 2008; E-mail: hashimi@umich.edu

Internal motions occurring on microsecond-to-millisecond time scales play essential roles in the functions of nucleic acids.^{1,2} Relaxation dispersion NMR spectroscopy is one of few techniques that can be used to site-specifically quantify these motions.^{3,4} $R_{1\rho}$ carbon relaxation dispersion has provided unique insights into such site-specific processes in nucleic acids,^{5,6} although studies to date have employed effective radiofrequency (RF) fields in the range of 1–6 kHz, thus limiting the sensitivity to exchange processes occurring on microsecond time scales. Slower millisecond motions can in principle be accessed by Carr–Purcell–Meiboom–Gill (CPMG) relaxation dispersion experiments, but extensive C–C scalar coupling networks in the base and sugar moieties of nucleic acids can severely complicate these experiments.⁷ Current multidimensional relaxation dispersion experiments also remain prohibitively time-consuming for carrying out measurements at natural abundance, making it difficult to characterize exchange processes in a large class of functional dynamics found at chemically modified sites that are difficult to enrich isotopically.

Here we present a carbon $R_{1\rho}$ NMR experiment (Figure 1) that extends the range of accessible time scales to ~ 10 ms and can be

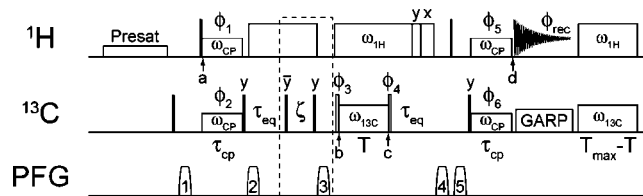


Figure 1. Selective ^{13}C $R_{1\rho}$ pulse sequence for quantifying microsecond-to-millisecond exchange in uniformly labeled and unlabeled nucleic acids. Briefly, proton magnetization is selectively transferred to the carbon spin using weak CW irradiation (ω_{CP}), where it is then allowed to relax under a variable offset and power spin-lock. The magnetization is returned to the proton for detection, and signal intensities are monitored as a function of spin-lock time, T , to determine $R_{1\rho}$ at a given offset and power. More details are provided in the Supporting Information.

applied to both uniformly labeled and unlabeled nucleic acid samples. Sensitivity to slower motions can be achieved through the appropriate use of ^1H decoupling and magnetization alignment schemes that permit use of significantly weaker RF fields (25–1000 Hz), as described by Palmer and co-workers⁸ and Kay and co-workers⁹ for amide ^{15}N in proteins. We have adapted the scheme introduced by Kay and co-workers for measuring nitrogen off-resonance $R_{1\rho}$ in proteins in designing the pulse sequence shown in Figure 1, which is optimized to measure off-resonance $R_{1\rho}$ for protonated carbons in uniformly labeled and unlabeled nucleic acids.

The experiment uses selective Hartmann–Hahn polarization transfers^{10–12} to excite specific spins of interest and collect data in a one-dimensional (1D) manner.^{9–14} This scheme is particularly

well-suited for nucleic acids, where chemical exchange is very often limited to a small number of residues in noncanonical regions, making it unnecessary to record full multidimensional experiments. The resultant ~ 100 -fold time savings makes it possible to comprehensively map out the carbon $R_{1\rho}$ dependence on the spin-lock amplitude (ω_1) and offset (Ω) and thus to thoroughly characterize the exchange process. It can also obviate the need for isotopic enrichment when working with concentrated nucleic acid samples (>2 mM). One-bond C–H scalar coupling ($^1J_{\text{CH}}$) evolution and cross-correlated relaxation between C–H dipole–dipole and carbon CSA during the relaxation period are efficiently suppressed by a strong ^1H continuous-wave (CW) field applied on the resonance of interest. Focusing on a single carbon resonance at a time makes it trivial to apply appropriately calibrated flip-angle pulses that align the magnetization along the effective magnetic field. These features make it possible to employ effective spin-lock fields as low as ~ 100 Hz. However, in uniformly labeled samples, appropriate experimental parameters (ω_1 , Ω) should be chosen to avoid additional C–C interactions (see the Supporting Information).^{15,16}

The A-site is a classic example of an RNA that uses conformational dynamics to carry out its function (insets in Figure 2). It decodes the mRNA message by dynamically flipping out two internal-loop adenines (A92 and A93, insets in Figure 2) once a proper codon–anticodon minihelix has been formed between the aminoacyl tRNA and mRNA.^{17,18} The A-site is also the target for many antibiotics that bind the internal loop and stabilize the flipped-out A92 and A93 conformation.

We used our experiment to probe the intrinsic dynamics in the A-site RNA internal loop, which may be important for decoding and adaptive recognition. In this unbound form, A92 and A93 adopt a looped-in conformation, with A93 forming a noncanonical hydrogen bond with A08.¹⁷ Monoexponential $R_{1\rho}$ decays were observed for carbon spin-lock fields in the range 90–3200 Hz (Figure S1). The strong offset and spin-lock-power dependence observed for the C2 R_2 of residue A08 (Figure 2a) and the C1' R_2 of residue A93 (Figure 2b) demonstrates existence of exchange at the internal loop. Importantly, this process would be difficult if not impossible to characterize by conventional methods, since the observed exchange is already nearly completely suppressed at spin-lock fields of ~ 1000 Hz (Figure 2a,b, right panels). In contrast to the internal loop, we did not observe any evidence of exchange at A10 in the canonical helix (Figure 2c and Figure S2).

The data from loop residues A08 and A93 could be fit simultaneously to a single exchange process with a time constant of $319 \pm 8 \mu\text{s}$ and a low-populated ($4.6 \pm 0.1\%$) “invisible” state. The measured time constant is short compared with decoding (~ 10 ms) and could reflect internal fluctuations that disrupt the A08–A93 base pair and thus enhance the looping out of A93. The dramatic time savings afforded by the new experiment also allowed us to

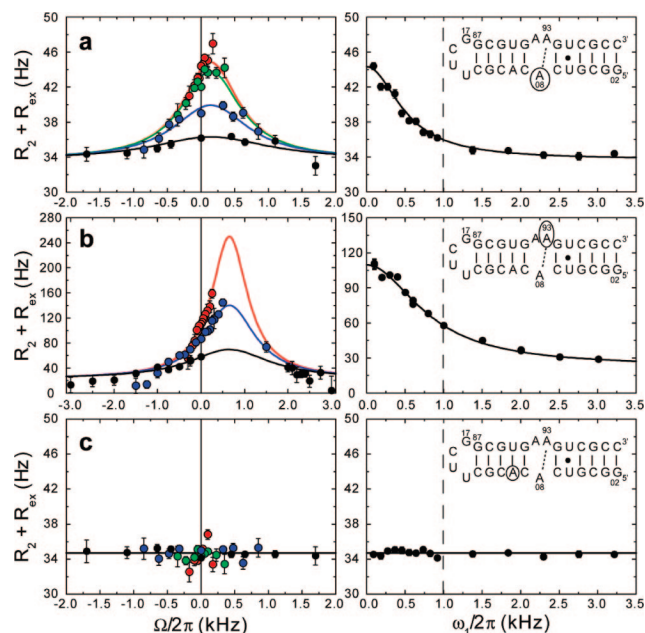


Figure 2. Characterization of decoding motions in the ribosomal A-site. The bacterial ribosomal A-site construct is shown in the insets of the right panels. (a–c) Relaxation dispersion profiles for (a) C2 in A08, (b) C1' in A93, and (c) C2 in A10. The left panels show the offset and power dependence of R_2 at spin-lock powers of (red) ~ 100 , (green) ~ 200 , (blue) ~ 500 , and (black) ~ 1000 Hz. The right panels show the corresponding on-resonance power dependence of R_2 . Dashed lines represent the approximate limits of $R_{1\rho}$ dispersion experiments measured using conventional 2D relaxation experiments. Solid lines represent the best-fit solution to two-site asymmetric chemical exchange (see the Supporting Information for details).

thoroughly map the offset dependence of R_2 for C2 in A08 and C1' in A93 and thus deduce the sign of the chemical shift difference ($\Omega = -\Delta\omega$; see the Supporting Information). This is not feasible using either on-resonance $R_{1\rho}$ or CPMG experiments alone at multiple static magnetic fields.¹⁹

The new experiment also makes possible the characterization of chemical exchange in unlabeled samples. This is particularly important for chemically modified molecules that cannot easily be isotopically enriched, including a wide range of DNA lesions in which motions are believed to play an important role in the recognition by repair enzymes.²⁰ To this end, we used our experiment to probe a DNA duplex containing a 1,N6-ethenoadenine (eA) lesion (see Figure 3a and the Supporting Information).

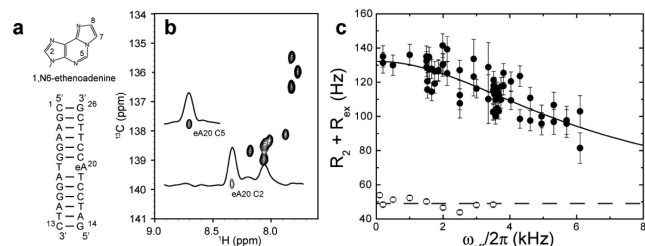


Figure 3. Quantification of chemical exchange in an unlabeled 1,N6-ethenoadenine damaged 26-mer DNA. (a) DNA sequence and chemical structure of the eA base. (b) 2D ^1H – ^{13}C correlation spectrum of the DNA sample at 14.4 T and 25 °C with 1D overlays to illustrate the sensitivity and selectivity of the pulse sequence in Figure 1. (c) Effective-field dependence of $R_2 + R_{\text{ex}}$. Data with errors >15 Hz have been omitted for clarity (Figure S3c). A sequence where eA20 is replaced with an adenine was used as a control (open symbols, C8 spin of A20). See the Supporting Information for details.

This allowed us for the first time to use relaxation dispersion to quantify dynamic exchange at a damaged DNA site.

Well-resolved C2H2 and C5H5 resonances in eA (Figure 3b) with anomalously weak intensities (Figure S3a) provided ideal probes for measuring exchange at the damaged site. A small but significant offset and power dependence for R_2 was observed for C2 in eA20 (Figure 3c and Figure S3b), which was measured in a constant-time manner to further reduce the experiment time. In contrast, the power dependence for R_2 measured in an identical sample lacking the damaged base was negligible (Figure 3c, open symbols). Despite the relatively large intrinsic R_2 , which can be attributed to elevated viscosity due to the high DNA concentration (~ 5 mM), and the very fast time scale of the exchange, the time constant for the eA20 exchange process could be reliably determined to be $26 \pm 8 \mu\text{s}$. This faster process may reflect transient destacking of eA20 that may help present the damaged base to repair enzymes.

In conclusion, we have presented an NMR experiment for measuring exchange dynamics over a broad range of time scales in both labeled and unlabeled nucleic acids. Use of very weak spin-lock fields affords a unique opportunity to quantify biologically important millisecond time scale motions in nucleic acids that have to date proven difficult to characterize reliably by conventional methods.

Acknowledgment. This work was supported by a National Science Foundation CAREER award (MCB 0644278) awarded to H.M.A. A.L.H. was supported by a Rackham Predoctoral Fellowship from the University of Michigan. E.N.N. was supported by a Rackham International Student Fellowship and a Rackham Faculty Research Grant from the University of Michigan. A.C.-N. was supported by a Sloan Fellowship from the Alfred P. Sloan Foundation.

Supporting Information Available: Details of sample preparation and assignment, the selective ^{13}C $R_{1\rho}$ pulse sequence, calculation of Hartman–Hahn conditions, and analysis of $R_{1\rho}$ offset and power dependence; figures illustrating monoexponential decays and qualitative detection of exchange from resonance intensities of A-site and eA DNA; and tables giving the Hartman–Hahn calculations for the A-site experiments and detailing the choice of chemical-exchange parameters for the A-site. This material is available free of charge via the Internet at <http://pubs.acs.org>.

References

- (1) Al-Hashimi, H. M.; Walter, N. G. *Curr. Opin. Struct. Biol.* **2008**, *18*, 321–329.
- (2) Furtig, B.; Buck, J.; Manoharan, V.; Bermel, W.; Jaschke, A.; Wenter, P.; Pitsch, S.; Schwalbe, H. *Biopolymers* **2007**, *86*, 360–383.
- (3) Palmer, A. G.; Massi, F. *Chem. Rev.* **2006**, *106*, 1700–1719.
- (4) Mittermaier, A.; Kay, L. E. *Science* **2006**, *312*, 224–228.
- (5) Shajani, Z.; Varani, G. *Biopolymers* **2007**, *86*, 348–359.
- (6) Latham, M. R.; Brown, D. J.; McCallum, S. A.; Pardi, A. *ChemBioChem* **2005**, *6*, 1492–1505.
- (7) Lundstrom, P.; Hansen, D. F.; Kay, L. E. *J. Biomol. NMR* **2008**, *42*, 35–47.
- (8) Massi, F.; Johnson, E.; Wang, C. Y.; Rance, M.; Palmer, A. G. *J. Am. Chem. Soc.* **2004**, *126*, 2247–2256.
- (9) Korzhnev, D. M.; Orekhov, V. Y.; Kay, L. E. *J. Am. Chem. Soc.* **2005**, *127*, 713–721.
- (10) Pelulessy, P.; Chiarparin, E.; Bodenhausen, G. *J. Magn. Reson.* **1999**, *138*, 178–181.
- (11) Pelulessy, P.; Chiarparin, E. *Concepts Magn. Reson.* **2000**, *12*, 103–124.
- (12) Ferrage, F.; Eykyn, T. R.; Bodenhausen, G. *ChemPhysChem* **2004**, *5*, 76–84.
- (13) Eykyn, T. R.; Ferrage, F.; Bodenhausen, G. *J. Chem. Phys.* **2002**, *116*, 10041–10050.
- (14) Ferrage, F.; Eykyn, T. R.; Bodenhausen, G. *J. Chem. Phys.* **2000**, *113*, 1081–1087.
- (15) Hansen, A. L.; Al-Hashimi, H. M. *J. Am. Chem. Soc.* **2007**, *129*, 16072–16082.
- (16) Bax, A.; Davis, D. G. *J. Magn. Reson.* **1985**, *63*, 207–213.
- (17) Fourmy, D.; Recht, M. I.; Blanchard, S. C.; Puglisi, J. D. *Science* **1996**, *274*, 1367–1371.
- (18) Fourmy, D.; Yoshizawa, S.; Puglisi, J. D. *J. Mol. Biol.* **1998**, *277*, 333–345.
- (19) Trott, O.; Palmer, A. G. *J. Magn. Reson.* **2002**, *154*, 157–160.
- (20) Yang, W. *Cell Res.* **2008**, *18*, 184–197.

JA8091399